Atmospheric Environment 77 (2013) 893–900

Contents lists available at SciVerse ScienceDirect

Atmospheric Environment

journal homepage: www.elsevier.com/locate/atmosenv

Role of atmospheric ammonia in particulate matter formation in Houston during summertime

Longwen Gong [a], Rafał Lewicki [b], Robert J. Griffin [a,*], Frank K. Tittel [b], Chantelle R. Lonsdale [c,d], Robin G. Stevens [c], Jeffrey R. Pierce [c,e], Quentin G.J. Malloy [a,f], Severin A. Travis [a,g], Loliya M. Bobmanuel [a,h], Barry L. Lefer [i], James H. Flynn [i]

[a] Department of Civil and Environmental Engineering, Rice University, Houston, TX, USA
[b] Department of Electrical and Computer Engineering, Rice University, Houston, TX, USA
[c] Department of Atmospheric Science, Dalhousie University, Halifax, NS, Canada
[d] Department of Geosciences, University of Massachusetts, Amherst, MA, USA
[e] Department of Atmospheric Science, Colorado State University, Fort Collins, CO, USA
[f] RTI International, Research Triangle Park, NC, USA
[g] Environmental Resources Management, Houston, TX, USA
[h] USA Environment, L.P., Houston, TX, USA
[i] Department of Earth and Atmospheric Sciences, University of Houston, Houston, TX, USA

HIGHLIGHTS

- Simultaneous measurements of gaseous and aerosol species were conducted.
- Atmospheric NH_3 contributed to increases in measured particle mass and measured/modeled particle number concentrations.
- NH_4^+ existed in the form of $(NH_4)_2SO_4$ and NH_4HSO_4; NH_4NO_3 and NH_4Cl formation was suppressed in summer.

ARTICLE INFO

Article history:
Received 4 December 2012
Received in revised form
24 April 2013
Accepted 30 April 2013

Keywords:
Ammonia
Particulate matter
Gas-particle partitioning
Aerosol nucleation

ABSTRACT

Simultaneous high-time-resolution measurements of atmospheric NH_3, HNO_3, soluble gas-phase chloride, and aerosol species were made in Houston, TX, from August 5, 2010 to August 9, 2010. Gaseous NH_3 was measured using a 10.4-μm external cavity quantum cascade laser-based sensor employing conventional photo-acoustic spectroscopy, while gaseous HNO_3 and HCl were sampled using a mist chamber–ion chromatograph (IC) system. Particle chemical composition was determined using a particle-into-liquid-sampler–IC system. There was a large amount of variability in the gas phase mixing ratios of NH_3 (3.0 ± 2.5 ppb), HNO_3 (287.4 ± 291.6 ppt), and HCl (221.3 ± 260.7 ppt). Elevated NH_3 levels occurred around mid-day when NH_4^+ (0.5 ± 1.0 μg m^{-3}) and SO_4^{2-} (4.5 ± 4.3 μg m^{-3}) also increased considerably, indicating that NH_3 likely influenced aerosol particle mass. By contrast, the formation of NH_4NO_3 and NH_4Cl was not observed during the measurements. Point sources (e.g., power plant and chemical plant) might be potential contributors to the enhancements in NH_3 at the measurement site under favorable meteorological conditions. Increased particle number concentrations were predicted by the SAM-TOMAS model downwind of a large coal-fired power plant when NH_3 emissions (based on these measurements) were included, highlighting the potential importance of NH_3 with respect to particle number concentration. Separate measurements also indicate the role of NH_3 in new particle formation in Houston under low-sulfur conditions.

1. Introduction

Ammonia (NH_3) is widely present in the atmosphere due to many anthropogenic and natural sources (Clarisse et al., 2009), usually at trace concentration levels ranging from parts per trillion (ppt) to parts per billion (ppb). Agricultural (e.g., fertilizer application and animal husbandry) (Mount et al., 2002; Rumburg et al., 2008) and industrial and motor vehicle (e.g., chemical production and traffic emission) (Kean and Harley, 2000; Hsieh and Chen, 2010) activities contribute to significant increases in local and/or regional NH_3 levels. In addition, National Emissions Inventory (NEI)

* Corresponding author. Tel.: +1 713 348 2093.
E-mail address: rob.griffin@rice.edu (R.J. Griffin).

1352-2310/$ – see front matter © 2013 Elsevier Ltd. All rights reserved.
http://dx.doi.org/10.1016/j.atmosenv.2013.04.079

air pollutant emissions trends data prepared by the United States Environmental Protection Agency (U.S. EPA) indicate that annual NH_3 emissions from the source category of electric utilities have risen continuously since 2005 (U.S. EPA, 2008).

Gaseous NH_3 can increase particulate matter (PM) mass concentrations through the formation of ammonium salts such as ammonium sulfate ($(NH_4)_2SO_4$), ammonium nitrate (NH_4NO_3), and ammonium chloride (NH_4Cl) via chemical reactions with sulfuric, nitric, and hydrochloric acids, respectively. Experiments also reveal that NH_3 plays a vital role in aerosol nucleation events (Kulmala et al., 2002). For example, McMurry et al. (2005) observed a positive correlation between number concentrations of nucleated particles and NH_3 in the sulfur-rich Atlanta atmosphere.

The resultant PM affects the Earth's radiation budget through direct and/or indirect effects and modifies the properties of clouds by serving as cloud condensation and/or ice nuclei (U.S. Climate Change Science Program, 2009). Epidemiological studies also have demonstrated a strong correlation between human exposure to PM and increased rates of respiratory and cardiovascular illness and other adverse human health effects (Pope et al., 2002; Pope and Dockery, 2006). Despite these implications for its negative impacts on air quality, NH_3 currently is not regulated under the National Ambient Air Quality Standards by the U.S. EPA. As a result, there are substantial uncertainties in spatial and temporal variations of NH_3 due to the scarcity of ground-based observations.

Conventional NH_3 studies primarily have focused on the measurements near source areas (e.g., farms) (Robarge et al., 2002; Ferm et al., 2005) using a bulk denuder technique with off-line analysis (e.g., ion chromatography (IC)) (Baek and Aneja, 2004; Wilson and Serre, 2007). Newly developed NH_3 instruments using laser spectroscopy and chemical ionization mass spectrometry have improved time resolution and detection limits and minimized human-induced errors (Nowak et al., 2007; Pogány et al., 2010). Meanwhile, relatively little previous work has investigated the effect of gas-particle partitioning of NH_3 and the interaction between NH_3 and acidic gaseous and particulate species due to a paucity of simultaneous datasets. In addition, information about NH_3 levels for the industrial and urban area of Greater Houston is still scarce. Nowak et al. (2010) conducted a 14-day aircraft measurement campaign including atmospheric NH_3 along the Houston Ship Channel (HSC) area during the second Texas Air Quality Study (TexAQS II). Gong et al. (2011) characterized the seasonal and diurnal patterns of gaseous NH_3 levels in Houston. According to a photochemical model, the estimated NH_3 mixing ratios for the Houston area are in the range of 1–15 ppb (Pavlovic et al., 2006).

The Toxics Release Inventory (TRI) of the U.S. EPA highlights the importance of NH_3 as an air pollutant in urban communities nationwide (U.S. EPA, 2010). Fig. 1(a) presents the total air toxics releases (20.8 million pounds) by species in the Houston–Sugar Land–Baytown metropolitan area according to the TRI in 2010 (U.S. EPA, 2010). It can be seen that NH_3 has the third largest individual magnitude of emissions after ethylene and propylene. Based on the NEI (U.S. EPA, 2008), agricultural and automobile activities are major contributors to gaseous NH_3 emissions. Fig. 1(b) summarizes the NEI NH_3 emissions (10.2 million pounds) by source categories specifically for Harris County, Texas in 2008 and indicates that on-road gasoline light duty vehicles and fertilizer application account for approximately 56% of the annual NH_3 emissions.

In order to examine the effects of NH_3 on air quality in Houston, measurements of gas-phase NH_3, nitric acid (HNO_3), soluble chloride (assumed to be hydrochloric acid (HCl)), and aerosol species were performed during the summer of 2010 by simultaneous on-line gas- and particle-phase instrumentation. In addition, NH_3 and particle number concentrations were measured synchronously during a one-month period in the summer of 2012. Finally, we performed model simulations aimed to elucidate the role that NH_3 plays in nucleation within power plant plumes in Houston.

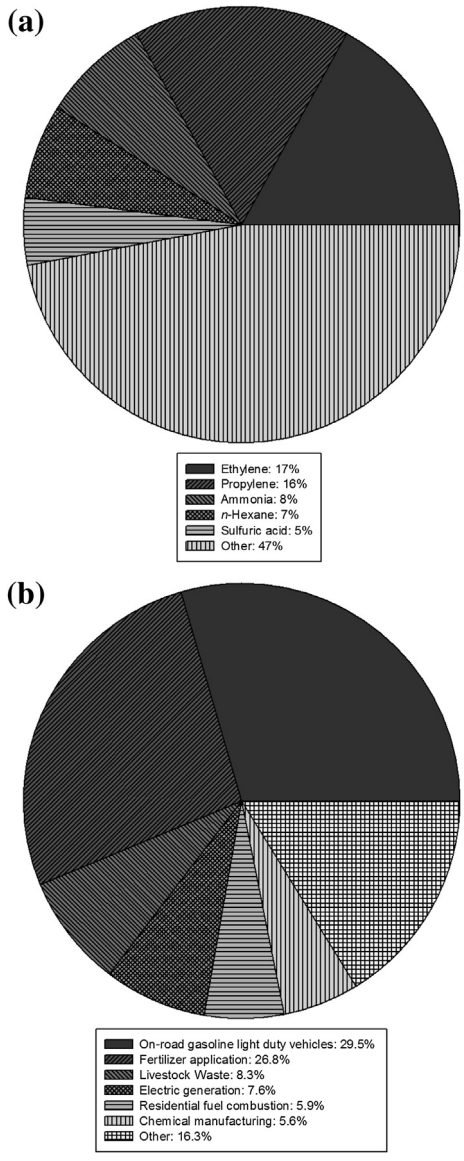

Fig. 1. (a) Annual total air toxics releases (20.8 million pounds) by species in the Houston–Sugar Land–Baytown metropolitan area (U.S. EPA, 2010); (b) Annual NH_3 emissions (10.2 million pounds) by source categories in Harris County, Texas (U.S. EPA, 2008).

2. Materials and methods

2.1. Sampling site

In this study, the simultaneous measurements of trace gases and particle chemical composition were carried out from August 5, 2010 to August 9, 2010. Although a five-day dataset is relatively limited, the total number of data points is large due to the highly time-resolved nature of the measurements and therefore can provide insight into air pollution episodes in an urban area potentially affected by industrial activities. All instruments were deployed in a trailer atop an 18-story (~65 m above ground level) building (North Moody Tower) located on the University of Houston (UH) main campus, which is influenced by many local and regional

emission sources such as highways, airports, and industrial facilities. Detailed information about this sampling site can be found in Lefer and Rappenglück (2010). Meteorological parameters (e.g., temperature and relative humidity) as well as mixing ratios of some important air pollutants (e.g., carbon monoxide (CO)) are measured regularly by the UH research group at this location (Lefer et al., 2010; Luke et al., 2010). All data were averaged into 1-h intervals solely for temporal consistency. A second one-month campaign was performed in July–August 2012 to investigate specifically the relationship between NH_3 and particle number concentration.

2.2. Gaseous species measurements

Gas-phase NH_3 was measured using a 10.4-μm external cavity quantum cascade laser-based sensor employing conventional photo-acoustic spectroscopy as described in detail in Gong et al. (2011). This optical sensor uses a state-of-the-art photo-acoustic cell that enables NH_3 detection limit at a sub-ppb level. The measurement accuracy is estimated to be ±7%. Gas-phase HNO_3 and HCl were measured using a mist chamber together with IC (Dionex, Model CD20-1), where the minimum detection limits of ppt levels were reached for a temporal resolution of 10 min with an uncertainty of ±10% (Dibb et al., 2004; Luke et al., 2010).

2.3. Aerosol species measurements

Particle chemical composition was measured using a particle-into-liquid-sampler (PILS) (BMI, Model 4002) coupled directly to two IC systems (Dionex, Model 1600) (Lee et al., 2003; Orsini et al., 2003). Mass concentrations (μg m^{-3}) of water-soluble inorganic components including ammonium (NH_4^+), sodium (Na^+), potassium (K^+), calcium (Ca^{2+}), magnesium (Mg^{2+}), sulfate (SO_4^{2-}), nitrate (NO_3^-), nitrite (NO_2^-) and chloride (Cl^-) in fine particle aerosols (with diameters smaller than 1 μm) were determined at 16-min intervals. The detection limit for measured ions is 100 ng m^{-3}, and the uncertainty of PILS–IC measurements is ±7% (Sorooshian et al., 2007). The continuous and real-time monitoring of particle number concentration (# of particles/volume of air) with a temporal resolution of one minute was performed using a condensation particle counter (TSI, Model 3772).

3. Results and discussion

3.1. Effect of NH_3 on particle mass concentrations

Fig. 2 presents a time series of hourly-averaged mixing ratios of gaseous NH_3 (3.0 ± 2.5 ppb (overall average ± one standard deviation)), HNO_3 (287.4 ± 291.6 ppt), HCl (221.3 ± 260.7 ppt), and CO (109.8 ± 22.4 ppb) and concentrations of particulate NH_4^+ (0.5 ± 1.0 μg m^{-3}), SO_4^{2-} (4.5 ± 4.3 μg m^{-3}), NO_3^- (0.3 ± 0.2 μg m^{-3}), and Cl^- (0.2 ± 0.1 μg m^{-3}) along with meteorological parameters. The NH_3 mixing ratios are a subset of the data considered by Gong et al. (2011). NH_3 levels were elevated around mid-day, when NH_4^+ and SO_4^{2-} also dramatically increased compared to other time periods of the measurements. This suggests that NH_3 played an important role in PM mass formation and that gas-particle conversion occurred when NH_3 was available, though SO_4^{2-} partitions to the aerosol phase regardless of NH_3 level. However, NO_3^- and Cl^- concentrations did not change significantly throughout the study period.

During these peaks, the wind mainly blew from the southwest in the direction of some point sources of NH_3 including a large coal-fired power plant (W. A. Parish) and chemical factories that are specified in the TRI (also verified by Hybrid Single-Particle Lagrangian Integrated Trajectory modeling (Draxler and Rolph, 2012)). The selective catalytic reduction (SCR) technique was installed to control nitrogen oxides (NO_x) emissions from Parish after 2004 (Peischl et al., 2010). Other unspecific/unidentified sources nearby the sampling site in that direction also might be potential contributors to elevated NH_3 levels.

Auxiliary data collected atop the North Moody Tower were used to assist in NH_3 source identification. For instance, primary pollutants such as CO emitted from automobile tailpipes can be used as indicators of vehicular emissions. Since the introduction of three-way catalytic converters, motor vehicles have contributed to elevated NH_3 levels in urban areas (Perrino et al., 2002; Kean et al., 2009) when NO_x is over-reduced inside the converters (Heck and Farrauto, 2001; Heeb et al., 2006; Ianniello et al., 2010). In the present work, nevertheless, no enhancements in CO were coincident with enhanced NH_3 around mid-day, indicating that motor vehicles are less likely to cause elevated NH_3 in Houston during the study period. This phenomenon might be related to the catalytic converter performance in summer; additional NH_3 sources also could obscure the NH_3–CO correlation, which was pronounced in winter (Gong et al., 2011).

During the five days of measurements, concurrent decreases in HNO_3 and HCl and concurrent increases in NO_3^- and Cl^- were not observed when NH_3 levels were elevated around mid-day, indicating that NH_4NO_3 and NH_4Cl were not formed in significant amounts. This hypothesis is confirmed by the very low saturation ratios ($<<1$) illustrated in Fig. 3. The saturation ratio is the partial pressure product ($P_{NH_3}P_{HNO_3}$ or $P_{NH_3}P_{HCl}$, in units of ppb^2) divided by the equilibrium constant ($K_{NH_4NO_3}$ or K_{NH_4Cl}, in units of ppb^2) that can be calculated using empirical equations (Pio and Harrison, 1987; Seinfeld and Pandis, 2006) based on the reversible formation of NH_4NO_3 and NH_4Cl (eqs (1) and (2)).

$$NH_3(g) + HNO_3(g) \leftrightarrow NH_4NO_3(s \text{ or } aq) \quad (1)$$

$$NH_3(g) + HCl(g) \leftrightarrow NH_4Cl(s \text{ or } aq) \quad (2)$$

Particulate NH_4NO_3 and NH_4Cl condense when the saturation ratio is larger than one, and they evaporate when the saturation ratio is smaller than one. This is in contrast to Nowak et al. (2010) who observed NH_4NO_3 formation during TexAQS II in HSC plumes with elevated NH_3 levels ranging from 5 to 80 ppb, probably due to the shift in the thermodynamic equilibrium towards the aerosol phase caused by very high NH_3 mixing ratios. High temperatures (30.1 ± 2.3 °C) likely do inhibit the formation of NH_4NO_3 and NH_4Cl because volatilization increases with temperature; by contrast, sulfate is considered essentially non-volatile (Bassett and Seinfeld, 1984). The Extended Aerosol Inorganics Model (E-AIM) also was employed, and it yielded similar results for the calculation of thermodynamic equilibrium/gas-particle partitioning using measurement data from this study (Clegg et al., 1998).

Comparable results have been reported previously by some urban-scale studies in other parts of the world. For example, in Barcelona, Pandolfi et al. (2012) conducted simultaneous measurements of gaseous NH_3 and aerosol species during summertime. It was found that the coefficients of determination between NH_4^+ and SO_4^{2-} and NO_3^- were 0.80 and 0.03, respectively, suggesting that NH_4NO_3 was not formed probably due to relatively high temperatures. In Central Taiwan, Lin et al. (2006) characterized NH_3, HNO_3, NH_4^+, and NO_3^-, and attributed lower NO_3^- concentrations in summer to the higher volatility levels of particulate NH_4NO_3. In Beijing, Meng et al. (2011) observed the decreased correlation between NH_4^+ and NO_3^- in summer compared to other seasons and noted that most of NH_4^+ in $PM_{2.5}$ is present as

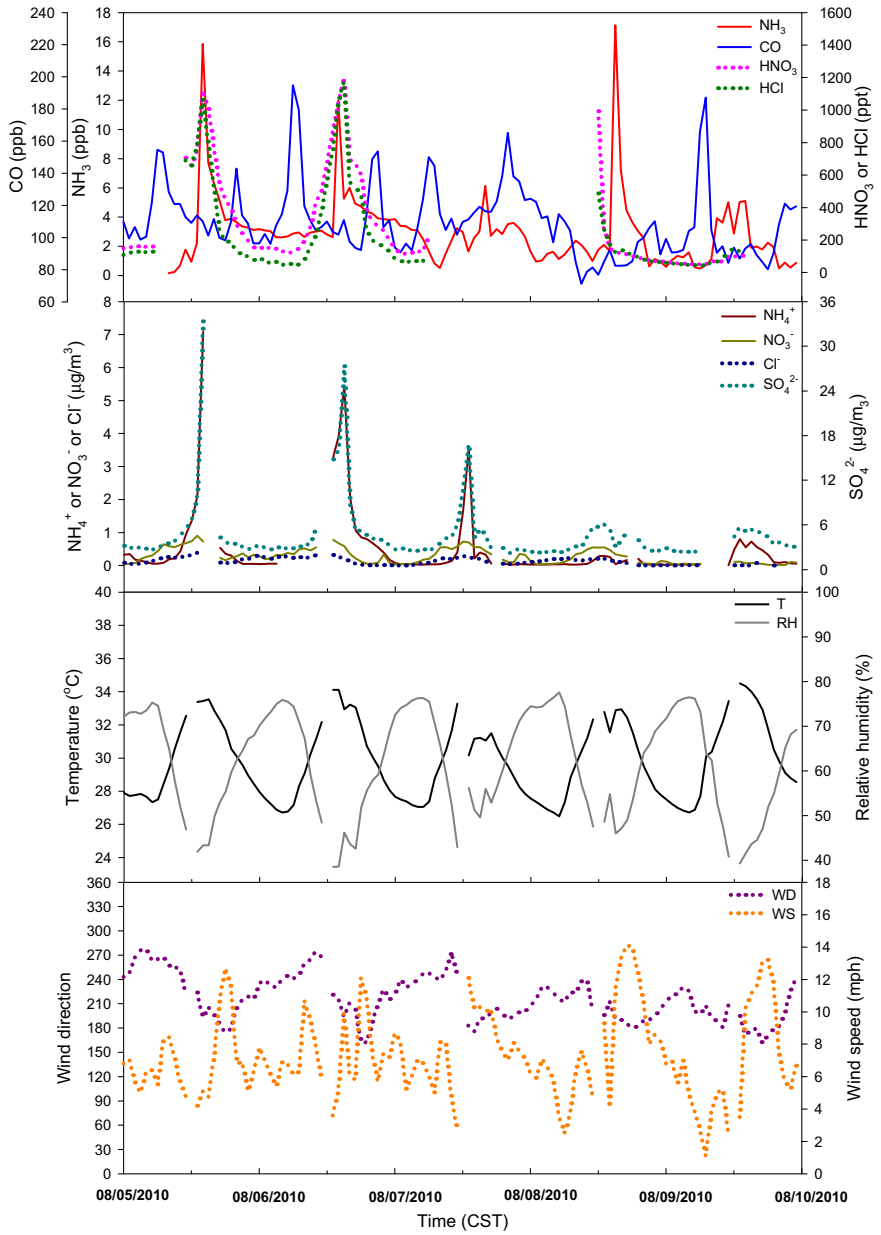

Fig. 2. Hourly-averaged mixing ratios of NH_3, HNO_3, HCl, and CO and concentrations of NH_4^+, SO_4^{2-}, NO_3^-, and Cl^-, as well as meteorological parameters during the 2010 measurements.

$(NH_4)_2SO_4$ during summertime. These findings support the hypothesis above for the lack of NH_4NO_3 in this study.

Table 1 summarizes the Pearson's correlation coefficients (R) between cations and anions during the measurement period, indicating that NH_4^+ is largely associated with SO_4^{2-} and that Na^+ and Mg^{2+} are closely correlated with NO_3^- and Cl^- based on the corresponding R values (>0.80). This could partially result from the different origin of air masses. For example, the concentrations of Na^+, Mg^{2+}, and Cl^- increased concurrently when southerly winds off the Gulf of Mexico were prevalent, indicating that air masses transported from the marine environment possibly affected the sampling site during those periods. Additionally, the slope (0.77) of the regression line between $[NH_4^+]$ and $[SO_4^{2-}]$ implies that $(NH_4)_2SO_4$ and ammonium bisulfate (NH_4HSO_4) might have co-existed.

A regression between molar concentrations of cations and anions yields a strongly linear relationship (Fig. 4, $R^2 = 0.96$; $p < 0.0001$; slope = 1.53), suggesting that ambient aerosols were likely acidic as a result of incomplete neutralization. However, the average value of the molar concentration ratio of gaseous NH_3 to total NH_3 (the sum of NH_3 and NH_4^+), also known as the gas fraction ($\sigma = 0.86 \pm 0.17$), suggests that NH_3 remained predominantly in the gas phase rather than the aerosol phase, as shown in Fig. 5, although sampled aerosols were ammonium-lean.

It is unlikely that aerosols that have achieved equilibrium are high in acid content when gaseous NH_3 is prevalent in the atmosphere. There may be aerosol cations such as aminium that are less likely to volatilize and that are not measured with the PILS–IC. However, if we assume that ambient aerosols are neutral and attribute all missing cations to aminium, the estimated required mixing ratio of gaseous amines following the example in

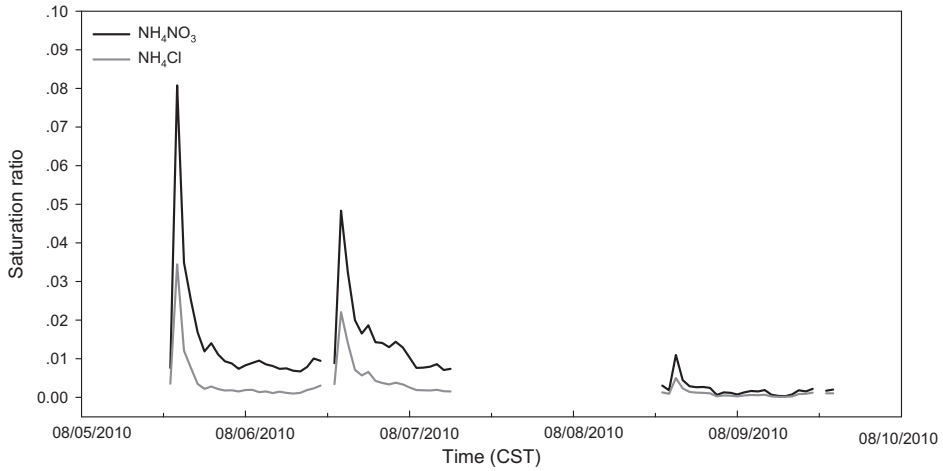

Fig. 3. Time series of the saturation ratios of NH_4NO_3 and NH_4Cl. $S = P_{NH_3}P_{HNO_3}/K_{NH_4NO_3}$ or $P_{NH_3}P_{HCl}/K_{NH_4Cl}$ where S is saturation ratio; P is partial pressure (in units of ppb); K is equilibrium constant (in units of ppb^2). $K = \exp[84.6 - 24220/T - 6.1\ln(T/298)]$ for NH_4NO_3. $K = \exp[2.2358\ln T - 2.13204{*}10^4\ T^{-1}{+}65.437516 - 8.167{*}10^{-3}\ T + 4.64383{*}10^{-7}\ T^2 - 1.10475{*}10^{-10}\ T^3]$ for NH_4Cl. where T is temperature in Kelvin.

Ge et al. (2011) is approximately 55 ppb, an unrealistically large value.

It has been shown that it can take several hours for atmospheric fine particles including ammonium salts to achieve equilibrium (Wexler and Seinfeld, 1992; Meng and Seinfeld, 1996), that coatings can cause mass transfer limitations with respect to ammonium sulfate particles (Chan and Chan, 2007), and that the presence of organic vapors can inhibit neutralization of sulfate aerosols by NH_3 (Liggio et al., 2011). While the data to prove that these phenomena occur in the Houston atmosphere do not exist for the current study, the possibility that one or more of them happen in Houston increases the likelihood of having non-neutral aerosols in the presence of excess gaseous NH_3.

It is also noted that the mean gas fractions for HNO_3 ($\sigma = 0.71 \pm 0.14$) and HCl ($\sigma = 0.72 \pm 0.24$) were larger than 0.5, as shown in Fig. 5, indicating they existed mainly in the gas phase. This observation may be attributed to the warm conditions during the measurements, which favor volatilization of NH_4NO_3 and NH_4Cl. In addition, Fig. 5 displays the molar concentration ratio of NH_3 to the sum of HNO_3 and HCl (11.3 ± 9.5) over the entire course of sampling, indicating that NH_3 was much more abundant than HNO_3 and HCl.

3.2. Effect of NH_3 on particle number concentrations

Nucleation of new particles frequently is observed in many locations throughout the world, even in the polluted atmosphere (e.g., Pittsburgh, St. Louis, Mexico City, Beijing, and the Po Valley) where the condensation sink is expected to be significant (Stanier et al., 2004; Hamed et al., 2007; Qian et al., 2007; Smith et al., 2008; Yue et al., 2010).

Aerosol nucleation and growth processes in coal-fired power plant plumes have been found to be great contributors to particle number concentrations near source regions (Brock et al., 2002). In Rochester, New York, Wang et al. (2011) observed largely decreased particle number concentrations (over a size range of 10–500 nm) attributable to the shutdown of a nearby large coal-fired power plant. Stevens et al. (2012) incorporated the TOMAS aerosol microphysics module (Adams and Seinfeld, 2002; Pierce and Adams, 2009) into the SAM Large-Eddy Simulation/Cloud Resolving model (Khairoutdinov and Randall, 2003) (SAM-TOMAS) and simulated significant nucleation and growth in the plume of two power plants (including the Parish plant), in agreement with aircraft measurements. Using the SAM-TOMAS to simulate the changes in NO_x and SO_2 emissions, Lonsdale et al. (2012) found enhanced particle nucleation and growth in the Parish plume as a result of the implementation of power plant emissions-control technologies (due to stronger NO_x controls than SO_2 controls). In the present work we also used this model to investigate how the excess NH_3 observed at an urban sampling site (presumably from the Parish power plant) may affect the nucleation and growth of particles in the plume. The model simulates the aerosol size distribution using 15 size bins segregated by dry mass per particle covering a size range from 3 nm to 10 μm and microphysical processes including coagulation, H_2SO_4 condensation, and nucleation

Table 1
Pearson's correlation coefficients (R) between cations and anions during the measurement period.

	SO_4^{2-}	NO_3^-	Cl^-	NO_2^-
NH_4^+	0.98	0.49	0.40	0.02
Na^+	0.58	0.90	0.94	0.28
Ca^{2+}	0.05	0.07	0.04	0.20
Mg^{2+}	0.41	0.81	0.91	0.07
K^+	0.41	0.36	0.15	0.38

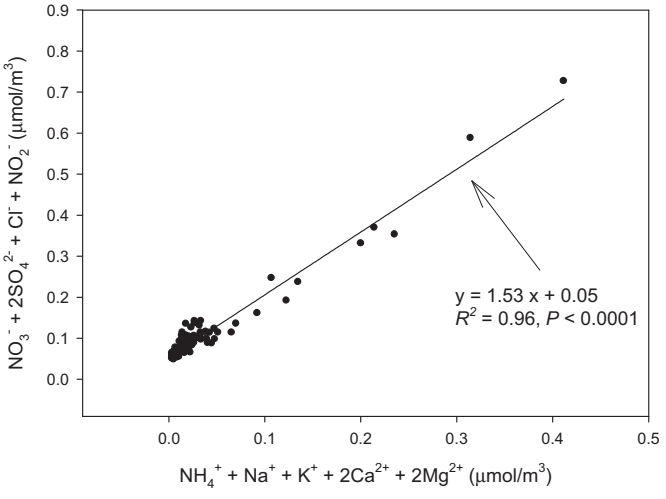

Fig. 4. Linear relationship between measured cations and anions.

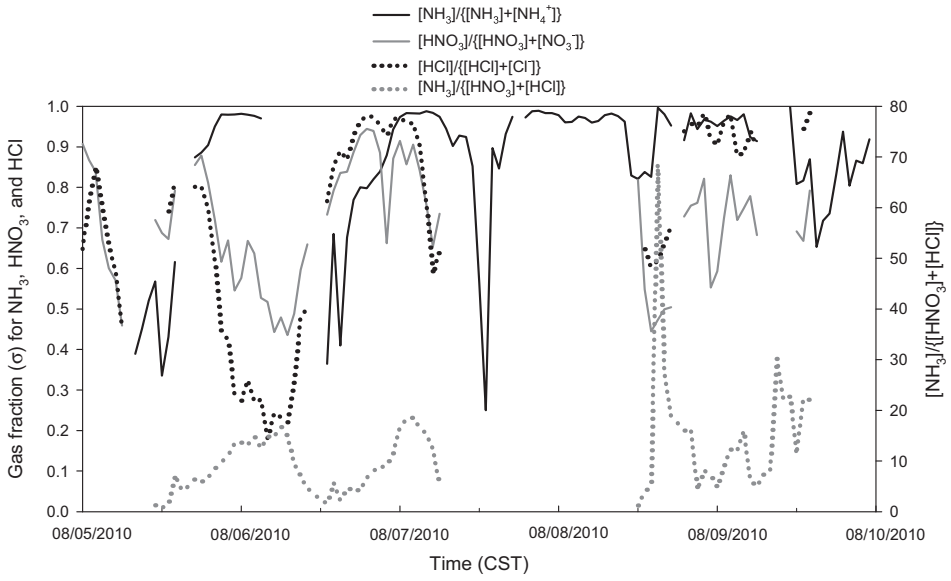

Fig. 5. Time series of gas fractions for NH_3, HNO_3 and HCl and of the ratio of NH_3 to the sum of HNO_3 and HCl.

(Stevens et al., 2012). Modeled H_2SO_4 vapor formation depends on sulfur dioxide (SO_2) and hydroxyl radical (OH) concentrations, and the OH concentrations in turn depend on the amount of sunlight and the NO_x concentrations.

NH_3 is considered to be a potentially important participant in aerosol nucleation and formation (Kulmala et al., 2000; Birmili et al., 2003; Kirkby et al., 2011). In order to evaluate the effects of NH_3 on particle number concentrations along the trajectory of power plant plumes, we hypothesize that elevated NH_3 levels originated from NH_3 slips at Parish, and we add NH_3 emissions from the plant to the SAM-TOMAS simulations, although relevant data from simultaneous measurements of particle number concentrations are not available as direct evidence for the 2010 campaign. Two ternary (H_2SO_4–H_2O–NH_3) nucleation schemes, Merikanto et al. (2006) and Napari et al. (2002) (which is scaled by a factor of 10^{-5} to better agree with observations (Westervelt et al., 2011)), are tested in SAM-TOMAS.

Fig. 6 shows twelve simulations from SAM-TOMAS under various environmental conditions. It shows the number of new particles in the plume normalized by the SO_2 emitted as a function of the distance downwind from the plant. Both schemes were run with 900 ppt and 0 ppt NH_3 background mixing ratios. In addition, three different NH_3 emission scenarios (high: 0.012 kg s^{-1}; medium: 0.007 kg s^{-1}; low: 0.0012 kg s^{-1}) were employed and tested based on the calculated range of NH_3 emission factors (82,500 to 825,000 lb yr^{-1}) from Parish based on vendor-estimated slip values (1–10 ppm) (Electric Power Research Institute, 2009). In all simulations, the number of new particles reaches a maximum near 10 km downwind; beyond this point, concentrations decrease because coagulation rates exceed nucleation rates. It can be seen that NH_3 emissions are very important for new particle formation, especially in the simulations in which background NH_3 mixing ratios are low (i.e., the green and red lines show a large variation in nucleation between simulations with different NH_3 emission rates). When background NH_3 mixing ratios were larger, the simulated effect of NH_3 emissions on nucleation was more saturated and the predicted differences between NH_3 emission scenarios were smaller. Specifically, the fractional increases in particle concentrations between the low and high NH_3 emission simulations at 50 km downwind were 1.1 for Merikanto's nucleation scheme with 900 ppt NH_3 background mixing ratio, 2.0 for Merikanto's nucleation scheme with 0 ppt NH_3 background mixing ratio, 1.2 for Napari's nucleation scheme with 900 ppt NH_3 background mixing ratio, and 2.5 for Napari's nucleation scheme with 0 ppt NH_3

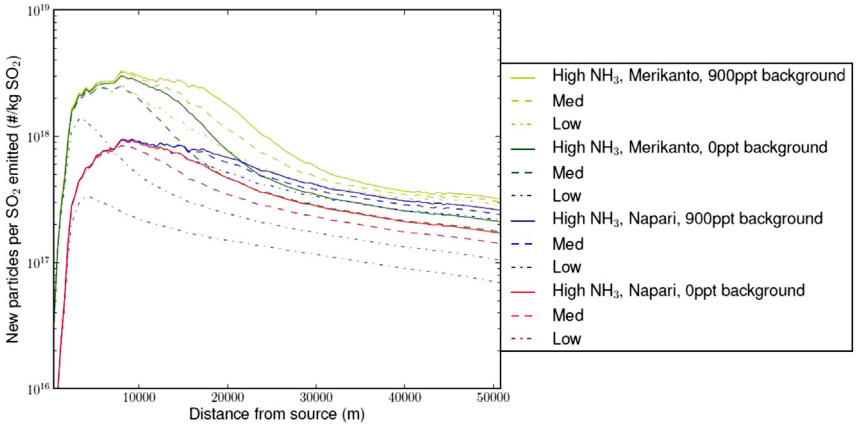

Fig. 6. The modeled number of particles formed by nucleation in the Parish plume per SO_2 mass emitted as a function of the distance downwind from the Parish plant.

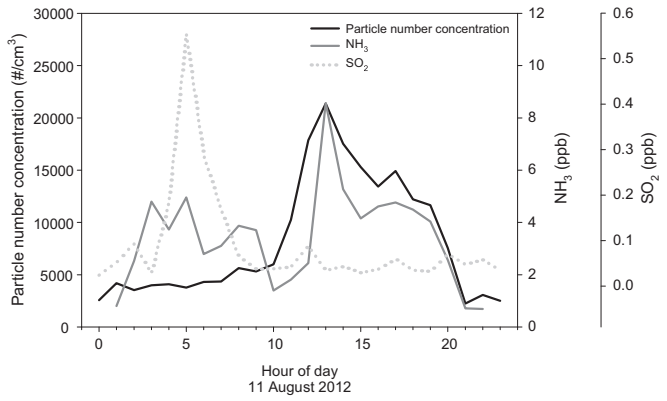

Fig. 7. Hourly variations in particle number concentration, NH_3, and SO_2 on August 11, 2012.

background mixing ratio, respectively. Larger NH_3 emissions accelerate aerosol nucleation in the simulations, as the system exhibits a high sensitivity to the amount of NH_3 slip, which emphasizes the significance of future NH_3 measurements in areas near power plants that utilize SCR. In addition, although Houston is currently in compliance with the mass-based $PM_{2.5}$ standards, efforts to characterize particle number concentration and size distribution synchronously with measurements of gaseous and particulate species are needed to better understand NH_3 impacts on both particle mass and number concentrations.

In order to further examine the link between atmospheric NH_3 and particle number concentration, simultaneous measurements of these two variables were conduct from July 19, 2012 to August 21, 2012 atop the North Moody Tower. Concurrent and significant increases in NH_3 mixing ratios and particle number concentrations were observed during some periods (an example of the episode on August 11, 2012 is shown in Fig. 7), although SO_2 levels were relatively and consistently low likely due to the lack of air masses transported from the power plant region. However, this underscores the importance of NH_3 as a potential precursor of aerosol particles, even in a sulfur-poor atmosphere.

4. Conclusions

Simultaneous measurements of gaseous and aerosol species were made in early August of 2010 in Houston, TX. Mixing ratios of trace gases showed a considerable amount of variability. Elevated NH_3 levels were synchronous with enhancements in NH_4^+ and SO_4^{2-} around mid-day, indicating the contribution of atmospheric NH_3 to particle mass concentrations. NH_4^+ existed in the form of $(NH_4)_2SO_4$ and NH_4HSO_4; however, the formation of NH_4NO_3 and NH_4Cl was not observed during the study period likely due to high ambient temperatures. Increased particle number concentrations were predicted by the SAM-TOMAS model downwind of a large coal-fired power plant when NH_3 emissions based on these measurements were included; observations indicate that NH_3 could be important in determining particle number concentrations, even without the presence of large amounts of sulfur. This study shows the significant effects of NH_3 on PM formation in the polluted Houston atmosphere, suggesting the importance and necessity of long-term or routine monitoring of aerosol precursors in the future.

Acknowledgments

This study was supported by the Mid-InfraRed Technologies for Health and the Environment (MIRTHE) Center and National Science Foundation (NSF) under grant No. EEC-0540832. Chantelle Lonsdale, Robin Stevens, and Jeffrey Pierce were funded by the Electric Power Research Institute (EPRI). Robin Stevens is supported by an NSERC PGS-D graduate fellowship. The authors gratefully acknowledge the NOAA Air Resources Laboratory (ARL) for the provision of the HYSPLIT transport and dispersion model and/or READY website (http://www.arl.noaa.gov/ready.php) and Drs. Anthony S. Wexler and Simon L. Clegg for the E-AIM model used in this publication. The authors also would like to thank Melanie Calzada and Kabindra Shakya for their help in data collection and preparation.

References

Adams, P.J., Seinfeld, J.H., 2002. Predicting global aerosol size distributions in general circulation models. Journal of Geophysical Research 107, 4370. http://dx.doi.org/10.1029/2001JD001010.

Baek, B.H., Aneja, V.P., 2004. Measurement and analysis of the relationship between ammonia, acid gases, and fine particles in eastern North Carolina. Journal of Air and Waste Management Association 54, 623–633.

Bassett, M.E., Seinfeld, J.H., 1984. Atmospheric equilibrium model of sulfate and nitrate aerosols – II. Particle size analysis. Atmospheric Environment 18, 1163–1170.

Birmili, W., Berresheim, H., Plass-Dulmer, C., Elste, T., Gilge, S., Wiedensohler, A., Uhrner, U., 2003. The Hohenpeissenberg aerosol formation experiment (HAFEX): a long-term study including size-resolved aerosol, H_2SO_4, OH, and monoterpenes measurements. Atmospheric Chemistry and Physics 3, 361–376.

Brock, C.A., Washenfelder, R.A., Trainer, M., Ryerson, T.B., Wilson, J.C., Reeves, J.M., Huey, L.G., Holloway, J.S., Parrish, D.D., Hübler, G., Fehsenfeld, F.C., 2002. Particle growth in the plumes of coal-fired power plants. Journal of Geophysical Research 107, 4155. http://dx.doi.org/10.1029/2001JD001062.

Chan, M.N., Chan, C.K., 2007. Mass transfer effects on the hygroscopic growth of ammonium sulfate particles with a water-insoluble coating. Atmospheric Environment 41, 4423–4433.

Clarisse, L., Clerbaux, C., Dentener, F., Hurtmans, D., Coheur, P.-F., 2009. Global ammonia distribution derived from infrared satellite observations. Nature Geoscience 2, 479–483. http://dx.doi.org/10.1038/ngeo551.

Clegg, S.L., Brimblecombe, P., Wexler, A.S., 1998. A thermodynamic model of the system $H^+ - NH_4^+ - SO_4^{2-} - NO_3^- - H_2O$ at tropospheric temperatures. Journal of Physical Chemistry A 102, 2137–2154.

Dibb, J.E., Scheuer, E., Whitlow, S.I., Vozella, M., 2004. Ship-based nitric acid measurements in the Gulf of Maine during New England Air Quality Study 2002. Journal of Geophysical Research 109, D20303. http://dx.doi.org/10.1029/2004JD004843.

Draxler, R.R., Rolph, G.D., 2012. HYSPLIT (HYbrid Single-particle Lagrangian Integrated Trajectory) Model Access via NOAA ARL READY Website. NOAA Air Resources Laboratory, Silver Spring, MD. http://ready.arl.noaa.gov/HYSPLIT.php.

Electric Power Research Institute, 2009. Estimating Ammonia Emissions from Stationary Power Plants. Technical Report #1017985.

Ferm, M., Marcinkowski, T., Kieronczyk, M., Pietrzak, S., 2005. Measurements of ammonia emissions from manure storing and spreading stages in polish commercial farms. Atmospheric Environment 39, 7106–7113.

Ge, X., Wexler, A.S., Clegg, S.L., 2011. Atmospheric amines – part II. Thermodynamic properties and gas/particle partitioning. Atmospheric Environment 45, 561–577.

Gong, L., Lewicki, R., Griffin, R.J., Flynn, J.H., Lefer, B.L., Tittel, F.K., 2011. Atmospheric ammonia measurements in Houston, TX using an external-cavity quantum cascade laser-based sensor. Atmospheric Chemistry and Physics 11, 9721–9733.

Hamed, A., Joutsensaari, J., Mikkonen, S., Sogacheva, L., Dal Maso, M., Kulmala, M., Cavalli, F., Fuzzi, S., Facchini, M.C., Decesari, S., Mircea, M., Lehtinen, K.E.J., Laaksonen, A., 2007. Nucleation and growth of new particles in Po Valley, Italy. Atmospheric Chemistry and Physics 7, 355–376.

Heck, R.M., Farrauto, R.J., 2001. Automobile exhaust catalysts. Applied Catalysis A: General 221, 443–457.

Heeb, N.V., Forss, A., Brühlmann, S., Lüscher, R., Saxer, C.J., Hug, P., 2006. Three-way catalyst-induced formation of ammonia – velocity- and acceleration-dependent emission factors. Atmospheric Environment 40, 5986–5997.

Hsieh, L.T., Chen, T.C., 2010. Characteristics of ambient ammonia levels measured in three different industrial parks in southern Taiwan. Aerosol and Air Quality Research 10, 596–608.

Ianniello, A., Spataro, F., Esposito, G., Allegrini, I., Rantica, E., Ancora, M.P., Hu, M., Zhu, T., 2010. Occurrence of gas phase ammonia in the area of Beijing (China). Atmospheric Chemistry and Physics 10, 9487–9503.

Kean, A.J., Harley, R.A., 2000. On-road measurement of ammonia and other motor vehicle exhaust emissions. Environmental Science and Technology 34, 3535–3539.

Kean, A.J., Littlejohn, D., Ban-Weiss, G.A., Harley, R.A., Kirchstetter, T.W., Lunden, M.M., 2009. Trends in on-road vehicle emissions of ammonia. Atmospheric Environment 43, 1565–1570.

Khairoutdinov, M.F., Randall, D.A., 2003. Cloud-resolving modeling of the ARM summer 1997 IOP: model formulation, results, uncertainties and sensitivities. Journal of the Atmospheric Sciences 60, 607–625.
Kirkby, J., et al., 2011. Role of sulphuric acid, ammonia and galactic cosmic rays in atmospheric aerosol nucleation. Nature 476, 429–433.
Kulmala, M., Pirjola, U., Mäkelä, J.M., 2000. Stable sulphate clusters as a source of new atmospheric particles. Nature 404, 66–69.
Kulmala, M., Korhonen, P., Napari, I., Karlsson, A., Berresheim, H., O'Dowd, C.D., 2002. Aerosol formation during PARFORCE: ternary nucleation of H_2SO_4, NH_3, and H_2O. Journal of Geophysical Research 107, 8111. http://dx.doi.org/10.1029/2001JD000900.
Lee, Y.-N., Weber, B., Ma, Y., Orsini, D., Maxwell-Meier, K., Blake, D., Meinardi, S., Sachse, G., Harward, C., Chen, T.-Y., Thornton, D., Tu, F.-H., Bandy, A., 2003. Airborne measurement of inorganic ionic components of fine aerosol particles using the particle-into-liquid sampler coupled to ion chromatography technique during ACE-Asia and TRACE-P. Journal of Geophysical Research 108, 8646. http://dx.doi.org/10.1029/2002JD003265.
Lefer, B., Rappenglück, B., 2010. The TexAQS-II radical and aerosol measurement project (TRAMP). Atmospheric Environment 44, 3997–4004.
Lefer, B., Rappenglück, B., Flynn, J., Haman, C., 2010. Photochemical and meteorological relationships during the Texas-II Radical and Aerosol Measurement Project (TRAMP). Atmospheric Environment 44, 4005–4013.
Liggio, J., Li, S.M., Vlasenko, A., Stroud, C., Makar, P., 2011. Depression of ammonia uptake to sulfuric acid aerosols by competing uptake of ambient organic gases. Environmental Science and Technology 45, 2790–2796.
Lin, Y.-C., Cheng, M.-T., Ting, W.-Y., Yeh, C.-R., 2006. Characteristics of gaseous HNO_2, HNO_3, NH_3 and particulate ammonium nitrate in an urban city of Central Taiwan. Atmospheric Environment 40, 4725–4733.
Lonsdale, C.R., Stevens, R.G., Brock, C.A., Makar, P.A., Knipping, E.M., Pierce, J.R., 2012. The effect of coal-fired power-plant SO_2 and NO_x control technologies on aerosol nucleation in the source plumes. Atmospheric Chemistry and Physics 12, 11519–11531.
Luke, W.T., Kelley, P., Lefer, B., Flynn, J., Rappenglück, B., Leuchner, M., Dibb, J.E., Ziemba, L.D., Anderson, C.H., Buhr, M., 2010. Measurements of primary trace gases and NO_Y composition in Houston, Texas. Atmospheric Environment 44, 4068–4080.
McMurry, P.H., Fink, M., Sakurai, H., Stolzenburg, M.R., Mauldin III, R.L., Smith, J., Eisele, F., Moore, K., Sjostedt, S., Tanner, D., Huey, L.G., Nowak, J.B., Edgerton, E., Voisin, D., 2005. A criterion for new particle formation in the sulfur-rich Atlanta atmosphere. Journal of Geophysical Research 110, D22S02. http://dx.doi.org/10.1029/2005JD005901.
Meng, Z., Seinfeld, J.H., 1996. Time scales to achieve atmospheric gas-aerosol equilibrium for volatile species. Atmospheric Environment 30, 2889–2900.
Meng, Z.Y., Lin, W.L., Jiang, X.M., Yan, P., Wang, Y., Zhang, Y.M., Yu, X.L., Jia, X.F., 2011. Characteristics of atmospheric ammonia over Beijing, China. Atmospheric Chemistry and Physics 11, 6139–6151. http://dx.doi.org/10.5194/acp-11-6139-2011.
Merikanto, J., Napari, I., Vehkamäki, H., Anttila, T., Kulmala, M., 2006. New parameterization of sulfuric acid–ammonia–water ternary nucleation rates at tropospheric conditions. Journal of Geophysical Research 112, D15207. http://dx.doi.org/10.1029/2006JD007977.
Mount, G.H., Rumburg, B., Havig, J., Lamb, B., Westberg, H., Yonge, D., Johnson, K., Kincaid, R., 2002. Measurement of atmospheric ammonia at a dairy using differential optical absorption spectroscopy in the mid-ultraviolet. Atmospheric Environment 36, 1799–1810.
Napari, I., Noppel, M., Vehkamäki, H., Kulmala, M., 2002. Parametrization of ternary nucleation rates for H_2SO_4–NH_3–H_2O vapors. Journal of Geophysical Research 107, 4381. http://dx.doi.org/10.1029/2002JD002132.
Nowak, J.B., Neuman, J.A., Kozai, K., Huey, L.G., Tanner, D.J., Holloway, J.S., Ryerson, T.B., Frost, G.J., McKeen, S.A., Fehsenfeld, F.C., 2007. A chemical ionization mass spectrometry technique for airborne measurements of ammonia. Journal of Geophysical Research 112, D10S02. http://dx.doi.org/10.1029/2006JD007589.
Nowak, J.B., Neuman, J.A., Bahreini, R., Brock, C.A., Middlebrook, A.M., Wollny, A.G., Holloway, J.S., Peischl, J., Ryerson, T.B., Fehsenfeld, F.C., 2010. Airborne observations of ammonia and ammonium nitrate formation over Houston, TX. Journal of Geophysical Research 115, D22304. http://dx.doi.org/10.1029/2010JD014195.
Orsini, D.A., Ma, Y., Sullivan, A., Sierau, B., Baumann, K., Weber, R.J., 2003. Refinements to the particle-into-liquid sampler (PILS) for ground and airborne measurements of water-soluble aerosol composition. Atmospheric Environment 37, 1243–1259.
Pandolfi, M., Amato, F., Reche, C., Alastuey, A., Otjes, R.P., Blom, M.J., Querol, X., 2012. Summer ammonia measurements in a densely populated Mediterranean city. Atmospheric Chemistry and Physics 12, 7557–7575.
Pavlovic, R.T., Nopmongcol, U., Kimura, Y., Allen, D.T., 2006. Ammonia emissions, concentrations and implications for particulate matter formation in Houston, TX. Atmospheric Environment 40, 538–551.
Peischl, J., Ryerson, T.B., Holloway, J.S., Parrish, D.D., Trainer, M., Frost, G.J., Aikin, K.C., Brown, S.S., Dubé, W.P., Stark, H., Fehsenfeld, F.C., 2010. A top–down analysis of emissions from selected Texas power plants during Tex-AQS 2000 and 2006. Journal of Geophysical Research 115, D16303. http://dx.doi.org/10.1029/2009JD013527.
Perrino, C., Catrambone, M., Di Menno Di Bucchianico, A., Allegrini, I., 2002. Gaseous ammonia in the urban area of Rome, Italy and its relationship with traffic emissions. Atmospheric Environment 36, 5385–5394.
Pierce, J.R., Adams, P.J., 2009. Uncertainty in global CCN concentrations from uncertain aerosol nucleation and primary emission rates. Atmospheric Chemistry and Physics 9, 1339–1356.
Pio, C.A., Harrison, R.M., 1987. The equilibrium of ammonium chloride aerosol with gaseous hydrochloric acid and ammonia under tropospheric conditions. Atmospheric Environment 21, 1243–1246.
Pogány, A., Mohácsi, Á., Jones, S.K., Nemitz, E., Varga, A., Bozóki, Z., Galbács, Z., Weidinger, T., Horváth, L., Szabó, G., 2010. Evaluation of a diode laser based photoacoustic instrument combined with preconcentration sampling for measuring surface–atmosphere exchange of ammonia with the aerodynamic gradient method. Atmospheric Environment 44, 1490–1496.
Pope, C.A., Burnett, R.T., Thun, M.J., Calle, E.E., Krewski, D., Ito, K., Thurston, G.D., 2002. Lung cancer, cardiopulmonary mortality, and long-term exposure to fine particulate air pollution. Journal of American Medical Association 287, 1132–1141.
Pope, C.A., Dockery, D.W., 2006. Health effects of the fine particulate air pollution: lines that connect. Journal of Air and Waste Management Association 56, 709–774.
Qian, S., Sakurai, H., McMurry, P.H., 2007. Characteristics of regional nucleation events in urban East St. Louis. Atmospheric Environment 41, 4119–4127.
Robarge, W.P., Walker, J.T., McCulloch, R.B., Murray, G., 2002. Atmospheric concentrations of ammonia and ammonium at an agricultural site in the southeast United States. Atmospheric Environment 36, 1661–1674.
Rumburg, B., Mount, G.H., Filipy, J., Lamb, B., Westberg, H., Yonge, D., Kincaid, R., Johnson, K., 2008. Measurement and modeling of atmospheric flux of ammonia from dairy milking cow housing. Atmospheric Environment 42, 3364–3379.
Seinfeld, J.H., Pandis, S.N., 2006. Atmospheric Chemistry and Physics: From Air Pollution to Climate Change. John Wiley, New York.
Smith, J.N., Dunn, M.J., VanReken, T.M., Iida, K., Stolzenburg, M.R., McMurry, P.H., Huey, L.G., 2008. Chemical composition of atmospheric nanoparticles formed from nucleation in Tecamac, Mexico: evidence for an important role for organic species in nanoparticle growth. Geophysical Research Letter 35, L04808. http://dx.doi.org/10.1029/2007GL032523.
Sorooshian, A., Lu, M.-L., Brechtel, F.J., Jonsson, H., Feingold, G., Flagan, R.C., Seinfeld, J.H., 2007. On the source of organic acid aerosol layers above clouds. Environmental Science and Technology 41 (13), 4647–4654.
Stanier, C.O., Khlystov, A.Y., Pandis, S.N., 2004. Ambient aerosol size distributions and number concentrations measured during the Pittsburgh Air Quality Study (PAQS). Atmospheric Environment 38, 3275–3284.
Stevens, R.G., Pierce, J.R., Brock, C.A., Reed, M.K., Crawford, J.H., Holloway, J.S., Ryerson, T.B., Huey, L.G., Nowak, J.B., 2012. Nucleation and growth of sulfate aerosol in coal-fired power plant plumes: sensitivity to background aerosol and meteorology. Atmospheric Chemistry and Physics 12, 189–206.
U.S. Climate Change Science Program, 2009. Atmospheric Aerosol Properties and Climate Impacts. In: Synthesis and Assessment Product 2.3.
U.S. EPA, 2008. National Emissions Inventory (NEI) Data Version 2. http://www.epa.gov/ttn/chief/net/2008inventory.html.
U.S. EPA, 2010. Toxics Release Inventory (TRI) National Analysis. http://www.epa.gov/tri/tridata/tri10/nationalanalysis/index.htm.
Wang, Y., Hopke, P.K., Chalupa, D.C., Utell, M.J., 2011. Effect of the shutdown of a coal-fired power plant on urban ultrafine particles and other pollutants. Aerosol Science and Technology 45, 1245–1249.
Westervelt, D.M., Riipinen, I., Pierce, J.R., Trivitayanurak, W., Adams, P.J., 2011. Formation and growth of nucleated particles: observational constraints on cloud condensation nuclei budgets. Atmospheric Chemistry and Physics Discussion 12, 11765–11822.
Wexler, A.S., Seinfeld, J.H., 1992. Analysis of aerosol ammonium nitrate: departures from equilibrium during SCAQS. Atmospheric Environment 26, 579–591.
Wilson, S.M., Serre, M.L., 2007. Use of passive samplers to measure atmospheric ammonia levels in a high-density industrial hog farm area of eastern North Carolina. Atmospheric Environment 28, 6074–6086.
Yue, D.L., Hu, M., Zhang, R.Y., Wang, Z.B., Zheng, J., Wu, Z.J., Wiedensohler, A., He, L.Y., Huang, X.F., Zhu, T., 2010. The roles of sulfuric acid in new particle formation and growth in the mega-city of Beijing. Atmospheric Chemistry and Physics 10, 4953–4960.